

Classical Stochastic Discrete Time Crystals

F. M. Gambetta,¹ F. Carollo,¹ A. Lazarides,² I. Lesanovsky,¹ and J. P. Garrahan¹

¹*School of Physics and Astronomy, University of Nottingham, Nottingham, NG7 2RD, United Kingdom and Centre for the Mathematics and Theoretical Physics of Quantum Non-equilibrium Systems, University of Nottingham, Nottingham NG7 2RD, UK*

²*Interdisciplinary Centre for Mathematical Modelling and Department of Mathematical Sciences, Loughborough University, Loughborough, LE11 3TU, UK*

(Dated: May 17, 2022)

We describe a possible general and simple paradigm in a classical thermal setting for discrete time crystals (DTCs), systems with stable dynamics which is subharmonic to the driving frequency thus breaking discrete time-translational invariance. We consider specifically an Ising model in two dimensions, as a prototypical system with a phase transition into stable phases distinguished by a local order parameter, driven by a thermal dynamics and periodically kicked. We show that for a wide parameter range a stable DTC emerges. The phase transition to the DTC state appears to be in the equilibrium 2D Ising class when dynamics is observed stroboscopically. However, we show that the DTC is a genuine non-equilibrium state. More generally, we speculate that systems with thermal phase transitions to multiple competing phases can give rise to DTCs when appropriately driven.

Introduction.— Discrete time crystals (DTCs) [1–20] have recently emerged as a novel form of non-equilibrium quantum matter. A time crystal is a system in which the time translation invariance of the dynamics is spontaneously broken asymptotically [21]. While time crystallinity is impossible in equilibrium states when the dynamics is time-homogeneous [22–24], it can emerge through spontaneous breaking of an underlying discrete time symmetry. Concrete examples have been found in closed quantum systems with time-periodic Hamiltonians (“Floquet” systems [25–27]) such as the π -spin glass and related models [2, 4–6, 8–10]. The usual setting in such unitary spin systems is that the dynamics is split between evolution with an interacting disordered Hamiltonian followed by a rotation of the spins. The usual Floquet heating towards an infinite temperature [28–30] state is avoided by exploiting localisation [31, 32] so spatio-temporal order can be established without fine tuning. For reviews see e.g. [33, 34].

The discovery of DTCs in unitary disordered Floquet systems raises numerous questions. Two important ones are the possibility of realising DTCs in clean quantum systems [7, 11, 12, 16, 17, 35], and whether DTCs can survive in the presence of dissipation [15, 36–49]. Studying these two issues is part of the more general search for an understanding of the range of mechanisms through which time crystalline order can be stabilised. In the case of quantum systems coupled to an external environment, the problem one faces is that of the natural tendency of dissipation to destabilise order [8, 9, 36, 44]. In this respect, several mean-field or fully connected model systems have been shown to display DTC behaviour with an appropriate engineering of the dissipative processes [38, 39, 41, 43, 45, 50], with some candidate open quantum systems argued to do the same away from mean-field [40, 44].

Here we consider another setting for DTCs, that of fully classical and thermal many-body systems. The generic scheme we propose is extremely simple, but to our knowledge has not been presented elsewhere before. The setup is that of a classical system with an equilibrium symmetry breaking transition - below we consider an Ising model in two dimensions (2D) as an obvious example - which is periodically driven. A period of the dynamics of duration τ consists of stochastic evolution under conditions such that asymptotically (i.e., if τ were to diverge) the symmetry-broken state would be stable,

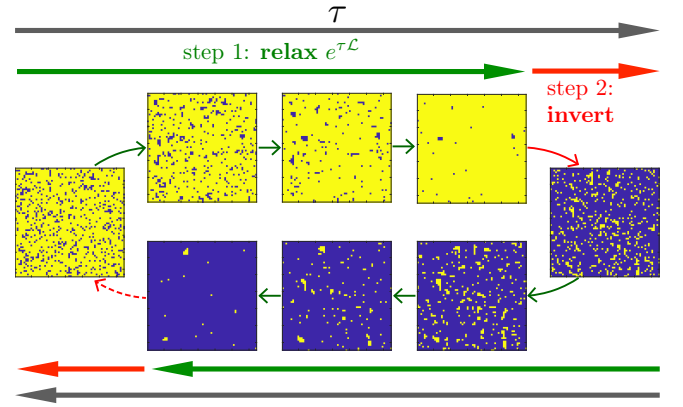


FIG. 1. **Dynamics of the driven Ising model under DTC conditions.** Starting a cycle from a magnetised state, domains of the opposite magnetisation (blue-dark/yellow-light indicate down/up, respectively) are annealed away under the evolution of duration τ generated by \mathcal{L} during step 1 of the protocol. Step 2 of the protocol randomly inverts most of the spins, leaving on average ε “mistakes”. These are subsequently annealed away in step 1 of the succeeding period. Due to the underlying symmetry breaking of the Ising model, only after two periods the original orientation of the spin profile is recovered. This gives rise to the period-doubling DTC.

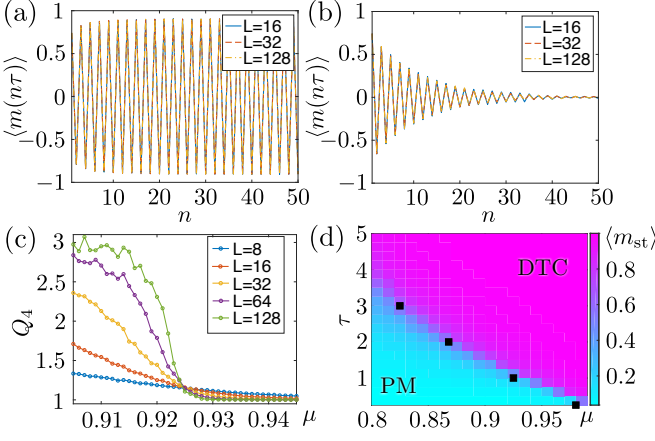


FIG. 2. **DTC phase transition.** (a) Magnetisation $m(n\tau)$ at the end of each cycle n for $(\tau, \mu) = (1, 0.95)$ from an initial $m_{in} = 0.8$. The persistent oscillations with a period of 2τ are indicative of a DTC. (b) Same for $(\tau, \mu) = (1, 0.85)$. In this case the oscillations get rapidly attenuated, indicative of the disordered time-homogeneous phase. (c) Binder cumulants Q_4 as a function of μ for $\tau = 1J^{-1}$. The crossing of the curves locates the critical point at $\mu_c \approx 0.925$. (d) Phase diagram of the driven Ising model as a function of μ and τ . The shading corresponds to the value of $\langle m_{st} \rangle$ in a system of linear size $L = 32$. The symbols give the location of $\mu_c(\tau)$ extracted from the crossing of the Binder cumulants at $\tau = \{0.25, 1, 2, 3\}$, cf. panel (c).

followed by a sudden random inversion of a fraction μ of the spins, see Fig. 1. We show that there exists a wide range of values of (τ, μ) in which a stable DTC emerges. This driven dynamics, when observed stroboscopically, leads to a non-equilibrium stationary state (NESS), in terms of which we construct the associated phase diagram as function of (τ, μ) . We show that despite the out-of-equilibrium nature of the dynamics, the transition from disorder to DTC order appears to be in the 2D Ising universality class.

Model and dynamical protocol.— We study a classical Ising model on a 2D square lattice of linear size L and periodic boundary conditions, with nearest neighbour couplings and no magnetic field. The energy function is

$$E(\sigma) \equiv -J \sum_{\langle i, j \rangle} \sigma_i \sigma_j, \quad (1)$$

where $\sigma_i = \pm 1$, sites are labelled by $i, j = \{1, \dots, L^2\}$, $\langle i, j \rangle$ indicates nearest neighbours, $\sigma = \{\sigma_i, \dots, \sigma_N\}$ with $N = L^2$ indicates a whole configuration of spins, and the coupling is ferromagnetic, i.e., $J > 0$. Below we set $J = 1$ for simplicity.

The dynamics is periodic [51] according to the following two-step protocol within each period, see Fig. 1:

1. The first step evolves the system for time τ (equal to the period) with a single spin-flip thermal dynamics which obeys detailed balance with respect

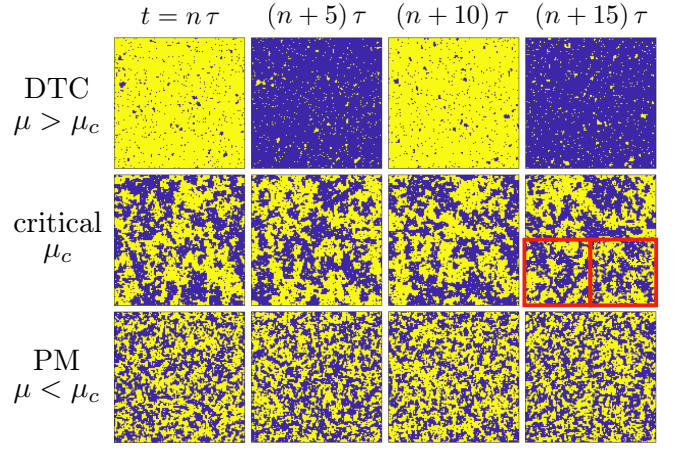


FIG. 3. **Stroboscopic trajectories.** Instantaneous configurations from representative trajectories under DTC conditions (top, $\mu = 0.95 > \mu_c$), near criticality (middle, $\mu = 0.9 \approx \mu_c$), and where the NESS is paramagnetic (bottom, $\mu = 0.8 < \mu_c$). Here, $\tau = 1J^{-1}$. We show a succession of snapshots for size 128×128 at times corresponding to odd and even cycles separated by 5τ , with $t = \tau \times \{1985, 1990, 1995, 2000\}$. The top row shows how the magnetisation alternates in the DTC. The inset at the bottom of the last panel in the middle row compares 64×64 (on the left) and 128×128 (on the right) configurations on the same scale to illustrate the self-similarity of the state at μ_c .

to the equilibrium Boltzmann distribution associated to energy function of Eq. (1) at temperature T . As we are interested in dynamics where a symmetry broken state is stable, we will restrict to $T = 0$ below.

2. The second step instantaneously inverts each spin with probability μ . When $\mu < 1$ not all spins are inverted, and we denote with $\varepsilon = 1 - \mu$ the “error” introduced in the inversion step.

This driven dynamics is described within a period by the evolution operator

$$\mathcal{F}_\tau \equiv \left[\prod_{i=1}^{L^2} (\varepsilon \mathbb{I}_i + \mu \hat{\sigma}_i^x) \right] e^{\mathcal{L}\tau}, \quad (2)$$

with $\hat{\sigma}_i^x$ and \mathbb{I}_i the x Pauli matrix and the identity matrix acting on the i -th spin, respectively. The rightmost factor implements step 1 above with

$$\mathcal{L} \equiv \sum_{i=1}^{L^2} (\hat{\sigma}_i^x - \mathbb{I}_i) \Gamma(\sigma) \quad (3)$$

the generator of zero-temperature Glauber dynamics [52–54]. Here, $\Gamma(\sigma) = \theta[E(\sigma) - E(\sigma_i)]$, where σ_i indicates the configuration obtained from σ by flipping the i -th spin, and $\theta(z)$ the Heaviside function. Therefore, only

moves that do not increase the energy are allowed. The leftmost factor in Eq. (2) implements step 2 above.

After a transient, the system reaches a time-periodic, non-equilibrium steady state. The dynamics depends on two parameters, the period τ and the rotated fraction of spins μ . To investigate the DTC phase transition it is convenient to consider as an observable the *stroboscopic time-staggered* magnetisation,

$$m_{\text{st}}(n) \equiv (-1)^n m(n\tau), \quad \text{with } n = 0, 1, \dots \quad (4)$$

where $m(t)$ denotes the total magnetisation per spin at time t ,

$$m(t) \equiv \frac{1}{L^2} \sum_{i=1}^{L^2} \sigma_i(t). \quad (5)$$

For large enough number of cycles we might expect that a stroboscopic NESS will be established. A natural order parameter is the average of the stroboscopic-time staggered magnetisation defined in Eq. (4) in this NESS,

$$\langle m_{\text{st}} \rangle = \lim_{N \rightarrow \infty} \frac{1}{N} \sum_{n=1}^N m_{\text{st}}(n). \quad (6)$$

Note that $\langle m_{\text{st}} \rangle$ corresponds to the usual order parameter used to identify DTC order [33, 34] given by the Fourier component of the magnetisation at half the driving frequency.

DTC state and phase transition.— We numerically investigate the dynamics given in Eq. (2) by using a continuous-time Monte Carlo algorithm [53, 55, 56] for the thermal part of the protocol. We study a range of system sizes and parameter values. In Figs. 2(a,b) we show the behaviour of the magnetisation at times which are multiples of the period, $m(n\tau)$ with $n = 0, 1, 2, \dots$, for $\tau = 1$ and two different values of μ . Figure 2(a) shows $m(n\tau)$ for $\mu = 0.95 > \mu_c \approx 0.925$. Here the system displays stable DTC oscillations with twice the period of the driving. The value $\mu_c \approx 0.925$ is our estimate at this τ of the transition point between an ordered DTC and a disordered driven paramagnet (see below for details). For a smaller value of $\mu = 0.85 < \mu_c$ (i.e., for a larger number of mistakes in the inversion) the oscillations in the magnetisation decay quickly with time, see Fig. 2(b), corresponding to the disordered (paramagnetic) phase (PM).

In terms of the staggered magnetisation, the disordered phase has $\langle m_{\text{st}} \rangle = 0$ while in the DTC phase $\langle m_{\text{st}} \rangle \neq 0$. For each value of τ we can therefore locate the phase transition point μ_c by means of Binder cumulants [53, 56]

$$Q_{2p} = \frac{\langle m_{\text{st}}^{2p} \rangle}{\langle |m_{\text{st}}^p| \rangle^2}, \quad (7)$$

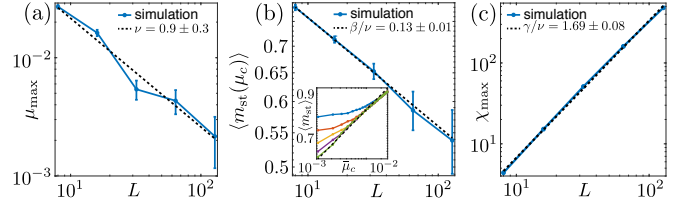


FIG. 4. **Critical exponents of the DTC transition obtained via finite size scaling.** (a) Plot of $\mu_{\text{max}} \sim L^{-1/\nu}$, corresponding to the point in which χ , see Eq. (8), takes its maximum value, $\chi(\mu_{\text{max}}) = \chi_{\text{max}}$, as a function L . The fit results in $\nu = 0.9 \pm 0.3$. The corresponding 2D Ising exponent is $\nu_{2D} = 1$. (b) Plot of $\langle m_{\text{st}}(\mu_c) \rangle \sim L^{-\beta/\nu}$. From the fit we get $\beta/\nu = 0.13 \pm 0.01$. Using the value of ν obtained in panel (a) we get $\beta = 0.12 \pm 0.04$. The 2D Ising exponent is $\beta_{2D} = 1/8$. Inset: plot of $\langle m_{\text{st}} \rangle$ as a function of $\bar{\mu}_c = (\mu - \mu_c)/\mu_c$ for the same sizes as in Fig. 2(c). Here, the slope of the fitting curve (black, dashed) has been fixed at value of β obtained from the main panel. (c) Maximum value of the susceptibility, $\chi_{\text{max}} \sim L^{\gamma/\nu}$, as a function of L . The fit leads to $\gamma/\nu = 1.69 \pm 0.08$. Using the result for ν from panel (a) we obtain $\gamma = 1.8 \pm 0.6$. The 2D Ising exponent is $\gamma_{2D} = 7/4$.

with $p \geq 2$. As Q_{2p} is size-independent at a transition point μ_c , the critical value μ_c is identified as the crossing point of the different curves in Fig. 2(c). The corresponding phase diagram in the (τ, μ) plane is shown in Fig. 2(d). For a given τ there is a $\mu_c(\tau)$ such that $\mu < \mu_c(\tau)$ corresponds to the disordered phase, while $\mu > \mu_c(\tau)$ to the DTC phase. $\mu_c(\tau)$ decreases with increasing τ as the longer annealing time allows for a larger error density before the DTC order becomes unstable.

Figure 3 shows configurations along representative trajectories in the various regimes of the dynamics. The top row corresponds to the DTC, $\mu > \mu_c$. Here the magnetisation at even and odd number of cycles alternates, displaying subharmonic behaviour. The bottom row corresponds to the paramagnetic stroboscopic NESS at $\mu < \mu_c$. Here, beyond fluctuations, there is no distinction between even and odd cycles, and discrete time symmetry remains unbroken. The middle row corresponds to conditions near criticality, $\mu \approx \mu_c$. The Inset to the last panel compares two different system sizes (on the same scale) illustrating self-similarity at the critical point.

Critical properties of the DTC transition.— The existence of a phase transition in the long-time state is evident from the susceptibility of the staggered magnetisation

$$\chi \equiv L^2 \left(\langle m_{\text{st}}^2 \rangle - \langle m_{\text{st}} \rangle^2 \right), \quad (8)$$

and from the correlation length ξ of the (equal-time) connected correlation function

$$C_{i,j}(t) \equiv \langle \sigma_i(t) \sigma_j(t) \rangle - \langle \sigma_i(t) \rangle \langle \sigma_j(t) \rangle, \quad (9)$$

extracted from the assumption that at large distances

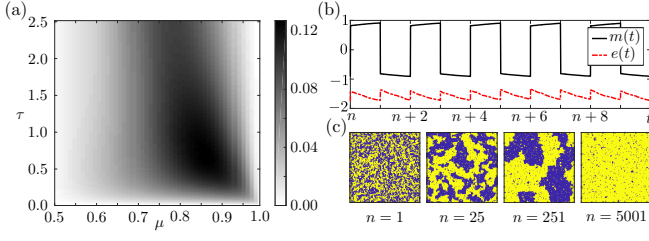


FIG. 5. **Non-equilibrium nature of the DTC.** (a) Sum of the absolute values of all elementary stationary currents q_{ij} for different values of the parameters (τ, μ) for $L = 3$. A non-zero value of this witnesses the non-equilibrium nature of the Floquet dynamics. (b) Time-dependent magnetisation $m(t)$ and energy $e(t) = J/L^2 \sum_{\langle i,j \rangle} \sigma_i(t) \sigma_j(t)$ (units J) for a system with $L = 128$. The value of n is chosen large enough so that the curves look stationary (in this case $n = 100$ is sufficient). The behaviour of both $m(t)$ (clearly displaying period-doubling) and of $e(t)$, which is not time-reversible, makes it evident that the process generating these trajectories has a non-equilibrium character. (c) Coarsening dynamics in the instantaneous configurations of the system for $t = \tau \times \{1, 25, 51, 5001\}$ with $m_{\text{in}} = 0.5$. In panels (b) and (c), $\tau = 1J^{-1}$ and $\mu = 0.95$.

$C_{i,j} \sim e^{-r_{ij}/\xi}$ with $r_{ij} \equiv |\mathbf{r}_i - \mathbf{r}_j|$ being the distance between spins i and j .

If the transition at μ_c is continuous then we expect to see critical scaling of $\langle m_{\text{st}} \rangle$, χ and ξ near it, that is,

$$\langle m_{\text{st}} \rangle \sim |\mu - \mu_c|^\beta, \quad \xi \sim |\mu - \mu_c|^{-\nu}, \quad \chi \sim |\mu - \mu_c|^{-\gamma}. \quad (10)$$

A finite-size scaling analysis in the stroboscopic NESS allows to extract the critical exponents, which are shown in Figure 4. The obtained values of (ν, β, γ) are close to those of the equilibrium 2D Ising model [57], despite the fact that in our case they correspond to a non-equilibrium phase transition.

Non-equilibrium nature of the DTC phase.—

There are several ways to support the latter statement. The first one, which sheds light on the origin of the phase transition, is to consider the analogy with a *two-temperature Ising model* [58–62]. Specifically, in the double limit of low error rate, $\varepsilon \ll 1$, and short length of the period, $\tau\Gamma(\boldsymbol{\sigma}) \ll 1$, we can write the evolution of the stroboscopic state by approximating the Floquet operator Eq. (2) as

$$\mathcal{F}_\tau \approx e^{\sum_i (\hat{\sigma}_i^x - \mathbb{I}_i) [\Gamma(\boldsymbol{\sigma}) + a'] \tau} \equiv e^{\tau \mathcal{L}_{\text{eff}}}. \quad (11)$$

Here we have used the identity $(1 - \varepsilon)\mathbb{I}_i + \varepsilon\hat{\sigma}_i^x = e^{a(\hat{\sigma}_i^x - \mathbb{I}_i)}$, where $a = -\log(1 - \varepsilon)^{1/2}$, and defined $a' = a/\tau$, so that for small ε one has $a'\tau \ll 1$. The generator \mathcal{L}_{eff} is that of a time-independent (i.e., non periodically driven) Glauber dynamics with composite transition rate $\Gamma(\boldsymbol{\sigma}) + a'$ corresponding to an Ising model in contact with two thermal baths [58–62]. When the temperatures of the

two baths are at either side of the critical temperature of the standard Ising model, this model is known to have a phase transition in the equilibrium Ising class [58–62]. In our case, one bath is at zero temperature, coming from the relaxation in step 1 of the driving protocol. The second bath is at infinite temperature, originating in the imperfect inversion in step 2, with a' setting the overall rate for the associated transitions. Thus, the DTC transition we find is, in the low error limit, analogous to that of the two-temperature Ising model which clearly has dynamics not obeying detailed balance when the two temperatures are different. This means that - at least for $\varepsilon \gtrsim 0$ - this DTC is also a NESS.

A second approach is to show that the dynamics due to Eq. (2) does not obey detailed balance and that the stroboscopic NESS produces entropy on average. If this is the case then there will be non-zero (stroboscopic) currents. A fundamental one would be the entropy production [63], but to estimate it one needs to know the transition probabilities between all pairs of configurations. These are contained in the operator \mathcal{F}_τ , see Eq. (2), but extracting them is impractical for large sizes. What we do is calculate all the average *elementary currents*, that is the currents $J_{\boldsymbol{\sigma} \rightarrow \boldsymbol{\sigma}'} \equiv \rho_{\boldsymbol{\sigma}} \mathcal{F}_{\boldsymbol{\sigma} \rightarrow \boldsymbol{\sigma}'} - \rho_{\boldsymbol{\sigma}'} \mathcal{F}_{\boldsymbol{\sigma}' \rightarrow \boldsymbol{\sigma}}$ between all pairs of configurations, $\boldsymbol{\sigma}$ and $\boldsymbol{\sigma}'$, where $\rho_{\boldsymbol{\sigma}}$ is the NESS of Eq. (2), and $\mathcal{F}_{\boldsymbol{\sigma} \rightarrow \boldsymbol{\sigma}'}$ are the corresponding probabilities for the transitions. This can be done exactly through exact diagonalisation of \mathcal{F}_τ for small sizes. Figure 5(a) gives the L_1 -norm of the current matrix, $\sum_{\boldsymbol{\sigma}, \boldsymbol{\sigma}'} |J_{\boldsymbol{\sigma} \rightarrow \boldsymbol{\sigma}'}|$ for a range of values of (τ, μ) , showing that except at the limits of $\tau = 0$ and $\mu = 1$ the average currents are non-vanishing. Furthermore, beyond the stroboscopic dynamics, trajectories of the system at all times are clearly non-reversible. This is seen in Fig. 5(b) where we show the energy and magnetisation for a representative DTC trajectory as a function of time.

Having shown that the long time state is a non-equilibrium one, we can ask whether the analogy with the 2D Ising model extends beyond the stroboscopic NESS. A simple test is to consider the dynamics starting from an initial state with zero magnetization (such as a quench from a random configuration). Figure 5(c) shows that under DTC conditions the stroboscopic dynamics exhibits *coarsening*, displaying progressive growth of domains of *both* magnetised states (before eventual collapse to one of the two in the last panel, which is a finite size effect). As the relaxation step of the protocol is standard Glauber Ising dynamics at zero temperature we could have expected coarsening only within a period, but the fact that it survives for long times despite the periodic driving is non-trivial, and constitutes another indication that the DTC state is robust.

Conclusions.— We have shown that a dynamic discrete time crystal can be obtained in a fully classical and thermal setting - and in the absence of disorder or any

form of classical localisation - as a symmetry breaking transition of a driven 2D Ising model. Our numerical results suggest that when observed stroboscopically, the phase transition in the non-equilibrium steady state is in the 2D Ising universality class. The mechanism for DTCs described here is simple and easily generalisable. For example, we expect that driven Potts models will lead to DTCs with periods larger than two. The simplicity of the scheme also suggest that it should be possible to observe these classical DTCs in experiments.

The research leading to these results has received funding from the European Research Council under the European Union's Seventh Framework Programme (FP/2007-2013)/ERC Grant Agreement No. 335266 (ES-CQUMA), and from EPSRC Grants No. EP/R04421X/1 and EP/N03404X/1. I.L. gratefully acknowledges funding through the Royal Society Wolfson Research Merit Award. The simulations used resources provided by the University of Nottingham High-Performance Computing Service.

-
- [1] K. Sacha, *Phys. Rev. A* **91**, 033617 (2015).
 - [2] V. Khemani, A. Lazarides, R. Moessner, and S. L. Sondhi, *Phys. Rev. Lett.* **116**, 250401 (2016).
 - [3] D. V. Else, B. Bauer, and C. Nayak, *Phys. Rev. Lett.* **117**, 090402 (2016).
 - [4] C. W. von Keyserlingk and S. L. Sondhi, *Phys. Rev. B* **93**, 245146 (2016).
 - [5] V. Khemani, C. W. von Keyserlingk, and S. L. Sondhi, *Phys. Rev. B* **96**, 115127 (2017).
 - [6] N. Y. Yao, A. C. Potter, I.-D. Potirniche, and A. Vishwanath, *Phys. Rev. Lett.* **118**, 030401 (2017).
 - [7] B. Huang, Y.-H. Wu, and W. V. Liu, *Phys. Rev. Lett.* **120**, 110603 (2018).
 - [8] S. Choi, J. Choi, R. Landig, G. Kucsko, H. Zhou, J. Isoya, F. Jelezko, S. Onoda, H. Sumiya, V. Khemani, C. von Keyserlingk, N. Y. Yao, E. Demler, and M. D. Lukin, *Nature* **543**, 221 EP (2017).
 - [9] J. Zhang, P. W. Hess, A. Kyprianidis, P. Becker, A. Lee, J. Smith, G. Pagano, I. D. Potirniche, A. C. Potter, A. Vishwanath, N. Y. Yao, and C. Monroe, *Nature* **543**, 217 EP (2017).
 - [10] W. W. Ho, S. Choi, M. D. Lukin, and D. A. Abanin, *Phys. Rev. Lett.* **119**, 010602 (2017).
 - [11] D. V. Else, B. Bauer, and C. Nayak, *Phys. Rev. X* **7**, 011026 (2017).
 - [12] A. Russomanno, F. Iemini, M. Dalmonte, and R. Fazio, *Phys. Rev. B* **95**, 214307 (2017).
 - [13] J. Rovny, R. L. Blum, and S. E. Barrett, *Phys. Rev. Lett.* **120**, 180603 (2018).
 - [14] J. Rovny, R. L. Blum, and S. E. Barrett, *Phys. Rev. B* **97**, 184301 (2018).
 - [15] S. Pal, N. Nishad, T. S. Mahesh, and G. J. Sreejith, *Phys. Rev. Lett.* **120**, 180602 (2018).
 - [16] W. C. Yu, J. Tangpanitanon, A. W. Glaetzle, D. Jaksch, and D. G. Angelakis, *Phys. Rev. A* **99**, 033618 (2019).
 - [17] R. E. Barfknecht, S. E. Rasmussen, A. Foerster, and N. T. Zinner, *Phys. Rev. B* **99**, 144304 (2019).
 - [18] F. Flicker, *SciPost Phys.* **5**, 1 (2018).
 - [19] N. Y. Yao, C. Nayak, L. Balents, and M. P. Zaletel, *arXiv:1801.02628* (2018).
 - [20] T. L. Heugel, M. Oscity, A. Eichler, O. Zilberberg, and R. Chitra, *arXiv:1903.02311* (2019).
 - [21] F. Wilczek, *Phys. Rev. Lett.* **109**, 160401 (2012).
 - [22] P. Bruno, *Phys. Rev. Lett.* **111**, 070402 (2013).
 - [23] P. Nozières, *EPL (Europhysics Letters)* **103**, 57008 (2013).
 - [24] H. Watanabe and M. Oshikawa, *Phys. Rev. Lett.* **114**, 251603 (2015).
 - [25] J. H. Shirley, *Phys. Rev.* **138**, B979 (1965).
 - [26] H. Sambe, *Phys. Rev. A* **7**, 2203 (1973).
 - [27] M. Grifoni and P. Hänggi, *Physics Reports* **304**, 229 (1998).
 - [28] L. D'Alessio and M. Rigol, *Phys. Rev. X* **4**, 041048 (2014).
 - [29] A. Lazarides, A. Das, and R. Moessner, *Phys. Rev. E* **90**, 012110 (2014).
 - [30] P. Ponte, A. Chandran, Z. Papić, and D. A. Abanin, *Ann. Phys.* **353**, 196 (2015).
 - [31] A. Lazarides, A. Das, and R. Moessner, *Phys. Rev. Lett.* **115**, 030402 (2015).
 - [32] P. Ponte, Z. Papić, F. m. c. Huveneers, and D. A. Abanin, *Phys. Rev. Lett.* **114**, 140401 (2015).
 - [33] R. Moessner and S. L. Sondhi, *Nature Physics* **13**, 424 EP (2017).
 - [34] K. Sacha and J. Zakrzewski, *Rep. Prog. Phys.* **81**, 016401 (2018).
 - [35] R. Schäfer, G. S. Uhrig, and J. Stolze, *arXiv:1904.12328* (2019).
 - [36] A. Lazarides and R. Moessner, *Phys. Rev. B* **95**, 195135 (2017).
 - [37] F. Iemini, A. Russomanno, J. Keeling, M. Schirò, M. Dalmonte, and R. Fazio, *Phys. Rev. Lett.* **121**, 035301 (2018).
 - [38] R. R. W. Wang, B. Xing, G. G. Carlo, and D. Poletti, *Phys. Rev. E* **97**, 020202 (2018).
 - [39] Z. Gong, R. Hamazaki, and M. Ueda, *Phys. Rev. Lett.* **120**, 040404 (2018).
 - [40] F. M. Gambetta, F. Carollo, M. Marcuzzi, J. P. Garrahan, and I. Lesanovsky, *Phys. Rev. Lett.* **122**, 015701 (2019).
 - [41] J. O'Sullivan, O. Lunt, C. W. Zollitsch, M. L. W. Thewalt, J. J. L. Morton, and A. Pal, *arXiv:1807.09884* (2018).
 - [42] K. Tucker, B. Zhu, R. J. Lewis-Swan, J. Marino, F. Jimenez, J. G. Restrepo, and A. M. Rey, *arXiv:1805.03343* (2018).
 - [43] B. Zhu, J. Marino, N. Y. Yao, M. D. Lukin, and E. A. Demler, *arXiv:1904.01026* (2019).
 - [44] A. Lazarides, S. Roy, F. Piazza, and R. Moessner, *arXiv:1904.04820* (2019).
 - [45] L. Dronner, R. Finsterhölzl, M. Heyl, and A. Carmele, *arXiv:1902.04986* (2019).
 - [46] B. Buča, J. Tindall, and D. Jaksch, *Nature Communications* **10**, 1730 (2019).
 - [47] M. Calvanese Strinati, L. Bello, A. Pe'er, and E. G. Dalla Torre, *arXiv:1901.07372* (2019).
 - [48] G. G. Carlo, L. Ermann, A. M. F. Rivas, and M. E. Spina, *Phys. Rev. E* **99**, 012214 (2019).
 - [49] L. Bello, M. Calvanese Strinati, E. G. Dalla Torre, and

- A. Pe'er, [arXiv:1901.06202](#) (2019).
- [50] H. Keßler, J. G. Cosme, M. Hemmerling, L. Mathey, and A. Hemmerich, [Phys. Rev. A](#) **99**, 053605 (2019).
- [51] For studies of other periodically driven Ising models see for example [64–66]. In Refs. [64–66] the driving is via a periodically oscillating magnetic field which, however, does not lead to DTC behaviour (but gives rise in certain instances to a transition in the Ising class to an ordered state where the average magnetisation oscillates with the period of the driving, so that the discrete time invariance is unbroken). Also note that the inversion step of Eq. (2) in our protocol cannot be realised by a time dependent change of the energy function (such as a with an oscillatory magnetic field).
- [52] R. J. Glauber, [Journal of Mathematical Physics](#) **4**, 294 (1963).
- [53] K. Binder and D. W. Heermann, *Monte Carlo Simulation in Statistical Physics*, edited by Springer-Verlag (Berlin Heidelberg, 2010).
- [54] P. L. Krapivsky, S. Redner, and E. Ben-Naim, *A Kinetic View of Statistical Physics* (Cambridge University Press, New York, 2010).
- [55] A. Bortz, M. Kalos, and J. Lebowitz, [Journal of Computational Physics](#) **17**, 10 (1975).
- [56] M. E. J. Newman and G. T. Barkema, *Monte Carlo Methods in Statistical Physics* (Oxford University Press, New York, 1999).
- [57] P. M. Chaikin and T. C. Lubensky, *Principles of Condensed Matter Physics* (Cambridge University Press, Cambridge, 1995).
- [58] P. Garrido, A. Labarta, and J. Marro, [J Stat Phys](#) **49**, 51 (1987).
- [59] H. W. J. Blote, J. R. Heringa, A. Hoogland, and R. K. Zia, [Journal of Physics A: Mathematical and General](#) **23**, 3799 (1990).
- [60] T. Tome, M. J. de Oliveira, and M. A. Santos, [Journal of Physics A: Mathematical and General](#) **24**, 3677 (1991).
- [61] P. Tamayo, F. J. Alexander, and R. Gupta, [Phys. Rev. E](#) **50**, 3474 (1994).
- [62] A. Achahbar, J. J. Alonso, and M. A. Muñoz, [Phys. Rev. E](#) **54**, 4838 (1996).
- [63] U. Seifert, [Rep. Prog. Phys.](#) **75**, 126001 (2012).
- [64] B. K. Chakrabarti and M. Acharyya, [Rev. Mod. Phys.](#) **71**, 847 (1999).
- [65] G. Korniss, C. J. White, P. A. Rikvold, and M. A. Novotny, [Phys. Rev. E](#) **63**, 016120 (2000).
- [66] H. Park and M. Pleimling, [Phys. Rev. E](#) **87**, 032145 (2013).